RF Plasma Synthesis of Amorphous AlN Powder and Films

Amorphous powder and thin films of aluminum nitride (AlN) are deposited in a parallel-plate RF plasma reactor starting from trimethylaluminum (TMA) and ammonia. Film deposition is favored at lower pressures and NH_3/TMA ratios; particle deposition occurs under higher pressures and NH_3/TMA ratios. Electron microscopy, x-ray diffraction, IR spectroscopy, and UV reflectance measurements are used for product characterization. Films of AlN grown at 250°C are transparent, pure, and have high UV reflectivity. AlN powder is amorphous and has a particle size of 10-20 nm and surface area of about 85 m^2/g. Amine impurities present in the as-deposited powder are removed by heat treatment at 600°C. The IR spectra of as-deposited powders do not show the characteristic Al-O bonding peak found in powders deposited by other methods.

M. David
S. V. Babu
D. H. Rasmussen
Department of Chemical Engineering
Clarkson University
Potsdam, NY 13676

Introduction

Aluminum nitride (AlN) is an excellent ceramic substrate material (Werdecker and Aldinger, 1984) for packaging of silicon very large scale integration (VLSI) devices due to its high thermal conductivity (as high as 320 W/mK), a coefficient of thermal expansion that matches with that of silicon over a wide temperature range (up to 1,000 K), a relatively low dielectric constant, and a nontoxic nature. Plasma-deposited powder is sintered at high temperatures to produce dense ceramic AlN bodies for use in VLSI devices. Plasma deposition is a vapor phase synthesis technique having the advantages of short reaction time, uniform size distribution, excellent product purity, minimum agglomeration, and high surface area. These are very desirable properties for the final product. For example, even small impurity levels in AlN powders drastically affect the properties of sintered material. Of particular importance is the role of oxygen. Thermal conductivity of AlN is reduced by a factor of two by the presence of a few weight percent of oxygen (Sakai et al., 1978). The low-pressure RF plasma synthesis described in this paper generates essentially oxygen-free nanometer-size amorphous AlN powder as well as thin films.

Plasmas can be operated either at low pressure (less than 100 Pa) or at higher pressures of 1,000 Pa to 1 atm (101.3 kPa). Low-pressure plasmas have low electron number densities and high electron temperatures (20,000 K or more) while the bulk gaseous temperatures are frequently less than 100°C. These plasmas are referred to as cold or nonequilibrium plasmas. As the pressure is increased, electrons lose their energy due to more frequent collisions with atoms, molecules, and free radicals, and equilibrate rapidly. Under these high temperature and equilibrium conditions, the electron temperature is not very different from that of the bulk gas (which is typically more than 1,000°C) and the plasma is referred to as a thermal or equilibrium plasma.

Plasma synthesis of ceramic powders is conventionally performed in thermal plasmas (Sheppard, 1987), where reactants are injected into the tail of a plasma torch and the product is collected after passing through a quenching tower. High adatom mobilities and high temperature phase transformations are responsible for the long range crystalline order observed in the thermal plasma synthesized product. However, sintering of such crystalline ceramic powder leads to large grain sizes that are unsuitable for applications involving submicron topographies. The thermal conductivity is also less than about 200 W/mK. In addition, such powders are susceptible to contamination from reactor walls. In any case, thermal plasmas are difficult to sustain, need high-power generators, and are subject to electrode erosion.

On the other hand, generation of particles in a cold RF plasma facilitates rapid phase change, frequently in a time scale much smaller than the time required for atomic rearrangement into a crystal lattice, yielding an amorphous product. The higher

---

Correspondence concerning this paper should be addressed to S. V. Babu.

degree of supersaturation and lower temperature in such plasmas favor nucleation over growth, resulting in extremely fine submicron particles. For example, very pure amorphous silicon nitride powder, 10–200 nm in size, with high surface area (35 m^2/g), has been deposited recently using silane and ammonia as reactants in an RF parallel-plate plasma reactor (Ho et al., 1989; Anderson et al., 1989, 1990). Reactors of this type need only compact low-power (less than 1,000 W) generators. Ceramic powder production in such reactors is an attractive alternative in small-volume applications where purity and uniformity are important, as in electronic ceramics, for example.

Indeed, it has been recently reported that ultrafine AlN powder (<100 nm) having a specific surface area of 30 m^2/g can be deposited in an RF plasma and that it can be sintered at temperatures as low as only 1,600°C (Baba et al., 1989). The sintered product has improved properties and lower defect densities due to the relatively small particle size and large surface area of the AlN powder. The RF plasma process described in this paper yields AlN clusters with superior characteristics—an average size of only 10–20 nm and a much larger surface area of about 85 m^2/g.

AlN is also an extremely promising passivating material for compound semiconductor technology. Compound semiconductors, like GaAs, have a higher electron mobility than Si, a direct band gap, and form heterojunctions. Nevertheless, progress in GaAs manufacturing technology has been slow. For example, development of a GaAs metal-insulator semiconductor field-effect transistor (MISFET) has not been successful, limited primarily by the absence of a good insulating or passivating film analogous to SiO_2 for Si technology. Development of AlN thin film deposition technology will prove immensely beneficial. Furthermore, the high reflectivity of AlN films in the short UV wavelength range (60–120 nm) makes them potentially useful for plasma fusion containment applications and as optical coatings over mirrors, windows, and lenses due to the high band gap of 6.2 eV.

Application of AlN for insulating or passivating films for GaAs MISFETs and packaging of VLSI devices require growth temperatures that do not exceed 500°C. However, most of the techniques for the growth of AlN films (Eichhorn and Rensch, 1982; Rensch and Eichhorn, 1983) require temperatures in the range of 1,100–1,200°C. At these temperatures single crystalline films are grown, but these are not epitaxial due to the lattice mismatch with substrate III–V materials. Hence a process that deposits pure, high-conductivity amorphous AlN films at low temperatures will be very attractive. Only recently, low-temperature ($T = 300°C$) plasma chemical vapor deposition (CVD) of AlN films has been reported (Hasegawa et al., 1987) using trimethylaluminum (TMA) and NH_3 as reactants with N_2 and H_2 as carrier gases in the pressure range of 133 to 400 Pa (1–3 torr). The plasma deposition process is investigated further here with the substrate maintained at only 250°C, using argon as the carrier gas with the pressure maintained at 40 Pa (0.3 torr).

It is the purpose of this paper to describe the low-temperature deposition of both films and powders of AlN from mixtures of trimethylaluminum and ammonia. The powders and films have been characterized by transmission electron microscopy (TEM), x-ray diffraction, IR spectroscopy, and UV reflectance measurements.

Experimental Method

A commercial parallel-plate plasma reactor (PlasmaTherm model 730/740) has been used for the deposition studies. A diagram of the reaction chamber is shown in Figure 1. RF power is supplied to the chamber through the upper electrode (0.28 m dia.), which is cooled by water/ethylene glycol coolant mixture circulated from a heat exchanger. Heating of substrates (up to 400°C) placed on the lower, grounded electrode is achieved by a resistance heater and controller. The reactor volume is 0.006 m^3, the active discharge volume being 0.0025 m^3. Four outlet ports (0.04 m dia.) arranged 90° apart on a 0.33 m dia. circle on the lower wall of the reactor lead the gases to a Roots blower backed by a mechanical pump. A capacitance manometer monitors the chamber pressure which is controlled by an exhaust valve and controller. The base pressure in the reactor is about 0.13 Pa (1 mtorr) and the combined desorption and air leak rate into the chamber is about 1.7×10^{-10} m^3/s (0.01 sccm).

A 600 W generator delivers RF power at 13.56 MHz through an automatic matching network to the reactor. The forward power is measured at the generator, the reflected power being negligible or zero in all experiments. The maximum power loss in the matching network is about 45 W.

The reactant species utilized for deposition are trimethylaluminum (TMA) (98% pure; Strem Chemicals) and ammonia (99.999% pure; Linde) or nitrogen (99.99% pure, dry grade; Linde). Hydrides of aluminum constitute the remaining 2% of the TMA. TMA is a liquid at room temperature, with a vapor pressure of 1,000 Pa at 25°C. Argon at atmospheric pressure is used as a carrier gas for transporting the TMA vapor from a bubbler to the reactor. Under the flow conditions used, the concentration of TMA in argon is about 1%. The flow rates of argon and ammonia or nitrogen are controlled by mass flow controllers. The reactant species enter a manifold before being fed into the reactor. However, powder deposition has led to blocking of the manifold. Subsequently the gas inlet has been modified to prevent such clogging. In the modified design, TMA and N_2 or NH_3 are introduced through separate gas lines that enter the reactor in directions that are orthogonal to each other.

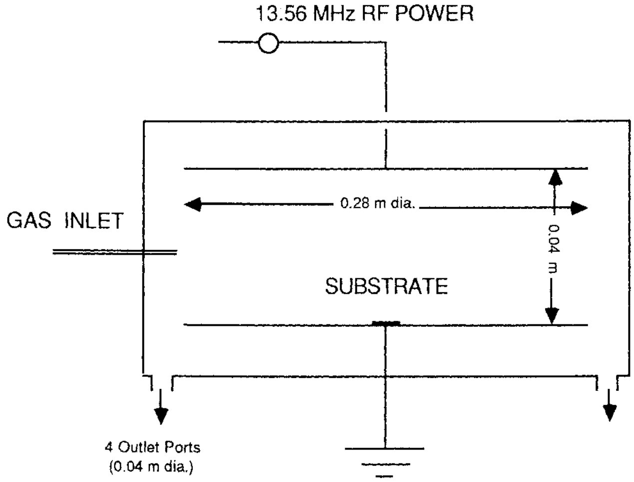

Figure 1. Parallel-plate plasma reactor used for deposition studies.

TMA and NH_3 enter reactor horizontally, in directions orthogonal to each other
Only one gas inlet is shown for clarity

Single-crystal (100) silicon wafers and precleaned glass microscope slides are used as substrates for thin films that are grown on the lower grounded electrode heated to 250°C. AlN powder generated in the gas phase is trapped in the centers of two vortices around which reactant gases swirl. Figure 2 diagrams the flow pattern along a cross section of the discharge volume between the two circular electrodes. Light scattered by the swirling cloud of particles generated in the glow discharge enables flow visualization. The two vortices are located symmetrically on either side of the ammonia gas inlet, as shown in Figure 2. The locations of the centers of the flow vortices depend upon the flow conditions (flow rate and pressure), which are adjusted to locate the vortices in the active discharge volume. The two vortices are always observed to be centered around the axis defined by the ammonia inlet. In the absence of the flow vortices, deposition occurs uniformly throughout the reactor volume and a significant fraction of deposited powder escapes if the ports are not covered with a porous filter. Although the presence of the vortices is not a requirement for powder formation, their occurrence is very convenient for collecting powder. Particles trapped in the vortices migrate by thermophoresis to the cooler, upper electrode. Fluffy lumps of deposited powder are scraped off the upper electrode and stored in a dessicator for further analysis.

A Siemens (model D500) x-ray diffractometer is used for diffraction studies. Deposited powder is dispersed in *n*-butanol by ultrasonification and centrifuged onto TEM grids for analysis in a JEOL transmission electron microscope (model JEM 1200 EX). IR spectra are obtained utilizing a Perkin Elmer spectrometer. UV reflectance is measured at Acton Research Corporation. Particle surface area is measured using the nitrogen BET method (Lowell, 1979).

Powder samples are heat treated after sealing in quartz ampoules evacuated to a pressure of 0.13 Pa (1 mtorr). The sealed ampoules are heated in a three-zone, split-tube furnace using a silicon carbide resistance heater. The time required for heating to 600°C is 15 min and the time for cooldown to room temperature is about 1h.

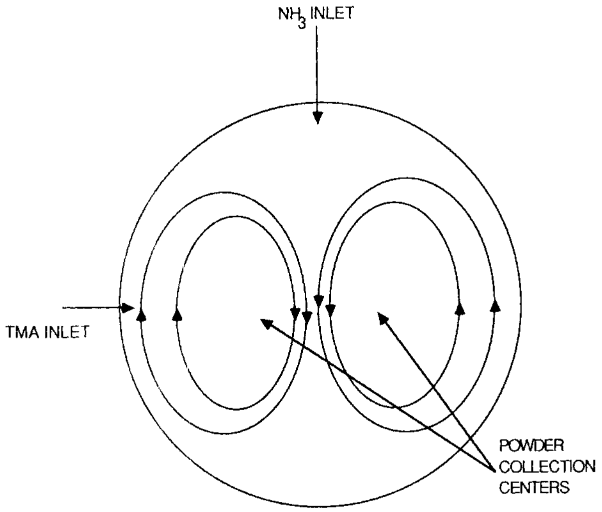

Figure 2. Horizontal cross section of active discharge volume showing vortices in which particles accumulate.

Circular electrode shown for reference
No vortices are observed in the direction of TMA flow

Table 1. Deposition Conditions with TMA and N_2 as Reactants

TMA/Ar flow rate	1.33×10^{-6} m^3/s (200 sccm)
N_2 flow rate	1.33×10^{-6} m^3/s (200 sccm)
Pressure	40.0 Pa (0.3 torr)
Plasma power	500 W
DC self-bias voltage	45 V
Deposition temp.	250°C

Results

TMA and nitrogen

Employing TMA and nitrogen as reactant species with the deposition conditions shown in Table 1 does not yield any visible deposit even after 90 min. Possible reasons for the lack of deposition are discussed later. Because of this negative result, ammonia is used as a reactant in all subsequent experiments.

TMA and ammonia

Transparent films showing colored interference fringes and white powder are simultaneously deposited in all deposition runs with ammonia and TMA. Among several process conditions investigated so far, such as feed gas composition and pressure, the film and cluster deposition rates are the highest for the process parameters listed in Table 2. However, increasing the total flow rate increases the deposition rate. Typical powder deposition rates are 800 mg/h and film deposition rates are 250 nm/h. The utilization rate of TMA for powder production is about 57% and about 4% for film formation. The film deposition rates are comparable to those of AlN films deposited by plasma-enhanced chemical vapor deposition (PECVD) from mixtures of aluminum bromide, nitrogen, hydrogen, and argon (Itoh et al., 1987) and from TMA and NH_3 with N_2 and H_2 as carrier gasses (Hasegawa et al., 1987). The flow vortices are not observed when argon is introduced without TMA vapor, as the particles that scatter light are absent. When the reactant gases are introduced in directions that are orthogonal to each other, the vortices as well as particle deposition occur mostly near the NH_3 inlet, while film deposition occurs mostly near the TMA inlet. Thus it is concluded that particle deposition requires higher NH_3/TMA ratios while film deposition is dominant at lower NH_3/TMA ratios.

Table 2. Deposition Conditions with TMA and NH_3 as Reactants

	Films	Powder
TMA/Ar flow rate	1.33×10^{-6} m^3/s (200 sccm)	1.33×10^{-6} m^3/s (200 sccm)
NH_3 flow rate	3.33×10^{-7} m^3/s (50 sccm)	2.0×10^{-6} m^3/s (300 sccm)
Pressure	40.0 Pa (0.3 torr)	133.3 Pa (1.0 torr)
Plasma power	500 W	600 W
DC self-bias voltage	125 V	80 V
Deposition temp.	250°C	<100°C

Film properties

Films deposited on silicon display color interference fringes while films deposited on microscope slides are transparent. The deposited films show excellent uniformity and do not reveal any morphological features even at a magnification of 20,000×. This is in contrast to films deposited by Itoh et al. (1987) which show a columnar structure.

X-ray diffraction studies of the deposited films do not yield any peaks, indicating that the films are amorphous. The IR spectrum of an as-deposited amorphous film is shown in Figure 3, in which the broad peak in the 600–700 cm^{-1} region represents Al-N bonding (Collins et al., 1967). The sharp peaks at 610 and 1,085 cm^{-1} correspond to the silicon substrate. The absence of any other structure is indicative of the excellent purity of the film.

The optical transparency of the deposited films is characteristic of large band gap materials. The extreme UV reflectance spectrum of an as deposited AlN film on silicon substrate is shown in Figure 4. The oscillatory nature of reflectance is due to interference effects. The amplitude of the oscillations decays exponentially with decreasing wavelength, the damping coefficient being proportional to the film absorption coefficient (Heavens, 1965). The presence of oscillations in the extreme UV is further evidence of a high band gap film (the photon energy corresponding to the highest wave number in the reflectance data shown in Figure 4 is 6.2 eV, which is the band gap of single-crystal AlN).

Powder properties

TMA–NH_3 plasma deposited powder is white and agglomerates into fluffy balls during deposition due to static charges developed in the glow discharge. Transmission electron microscopy reveals a particle size in the 10–20 nm range with a narrow size distribution devoid of any crystalline features, as seen in Figure 5. Samples of powder taken from the deposition chamber at different intervals of time (2, 5, 15, 25, 45 min) display virtually the same particle size. The invariant particle size implies that nucleation rather than growth is the dominant deposition mechanism, with the number of particles produced in the reactor increasing with time. When the particles are in thermal equilibrium with the plasma, their growth rate is small under the prevailing low-temperature conditions. Any growth in particle size is therefore limited to the period during which the particles approach equilibrium. The surface area of the as-deposited powder is measured by the BET method to be about $85 m^2/g$.

X-ray diffraction studies of the deposited powder reveal that it is amorphous, as in the case of films and in general agreement with the published results for RF plasma deposited silicon nitride powder (Ho et al., 1989). The presence of Al-N bonding in the powder is confirmed by the IR spectrum shown in Figure 6. The IR absorption spectrum is measured in the 400–4,000 cm^{-1} interval by mixing the powder into a KBr pellet. The absorption band centered around 670 cm^{-1} is attributable to Al-N bonding (Collins et al., 1967), while the broadening of the band is a result of the amorphous nature (Hasegawa et al., 1987). The absorption peak centered around 3,400 cm^{-1} is either due to O-H or N-H stretching modes (*Handbook of Chemistry and Physics,* 1985, p. F-199). However, the intensity of this peak diminishes upon heat treatment, Figure 7, without the generation of an Al-O peak at 460 cm^{-1}. Since oxygen readily converts aluminum nitride to aluminum oxide, the absence of any Al-O bonding in the heat-treated powder leads to the conclusion that the 3,400 cm^{-1} peak is due to N-H stetching vibration. The peaks at 1,550 and 1,650 cm^{-1}, whose intensity decreases significantly upon heat treatment, arise from amine groups (*Handbook of Chemistry and Physics,* 1985, p. F-199). Finally, the sharp 2,200 cm^{-1} peak, which broadens upon heat treatment, is due to Al-H bonding (Hasegawa et al., 1987).The IR spectrum of the AlN powder heat treated at 600°C for 6 h is shown in Figure 7. It contains the Al-N peak as its chief constituent, in addition to residual weak Al-H and N-H peaks. Heat treatment eliminates the amine impurities present in the as-deposited powder. The amine peaks are absent in the IR spectra of the films even though they are deposited only at a temperature of 250°C.

Discussion

Reaction between TMA and nitrogen does not lead to any visible deposit even after 90 min, consistent with the results of earlier investigations of AlN deposition by CVD (Eichhorn and Rensch, 1982; Rensch and Eichhorn, 1983) and PECVD

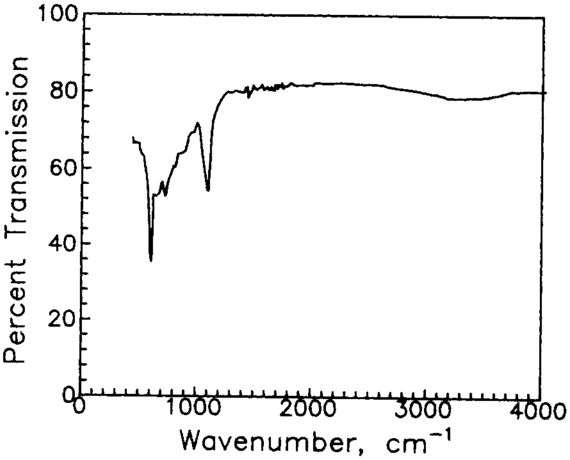

Figure 3. IR spectrum of an as-deposited aluminum nitride film.

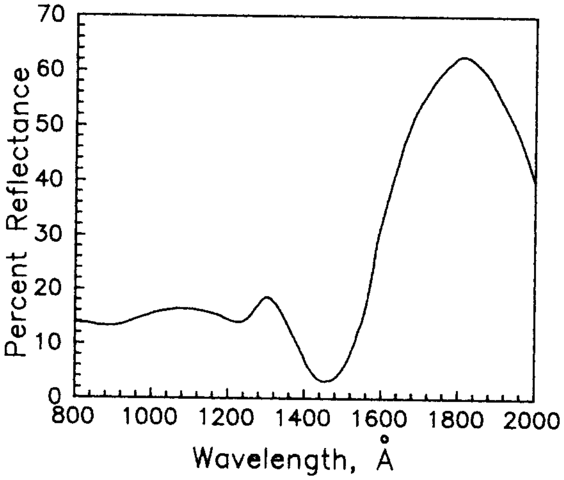

Figure 4. UV reflectance spectrum of an as-deposited aluminum nitride film.

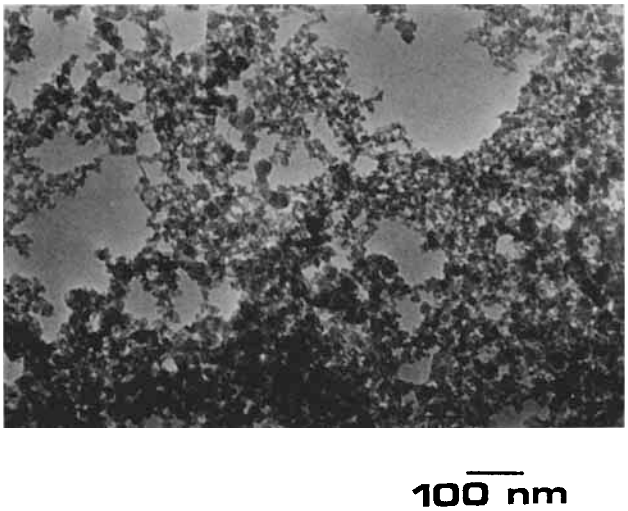

Figure 5. Transmission electron micrograph of as-deposited aluminum nitride powder.

(Hasegawa et al., 1987; Itoh et al., 1987). Itoh et al., for example, report that AlN deposition occurs only when H_2 is added to a mixture of $AlBr_3$ and N_2. Presumably, an abundance of NH_x-containing groups, where $x = 1$ or 2, is necessary for deposition of AlN. In plasma deposition processes, these radicals are formed by electron impact dissociation of reactant molecules. The dissociation may proceed in several ways:

$$\begin{array}{llll} NH_3 \rightarrow NH_2 & + H & & \Delta H^0 = 4.50\text{ eV} \\ NH_3 \rightarrow NH & + H_2 & & \Delta H^0 = 3.92\text{ eV} \\ NH_3 \rightarrow N & + H + H_2 & & \Delta H^0 = 7.67\text{ eV} \\ NH_2 \rightarrow NH & + H & & \Delta H^0 = 3.96\text{ eV} \\ NH \rightarrow N & + H & & \Delta H^0 = 3.75\text{ eV} \\ N_2 \rightarrow N & + N & & \Delta H^0 = 9.84\text{ eV} \end{array}$$

The standard enthalpy changes of the various dissociation reactions are calculated from the standard heats of formation (Hirose, 1986). The dissociation pathway for nitrogen requires a much higher energy than the pathways for ammonia dissociation. Hence, the concentration of NH_x species is likely to be significantly lower in nitrogen-TMA plasmas than in ammonia-TMA plasmas. Consequently, the deposition rate will be much lower when nitrogen is the reactant. Indeed, it has been observed to be negligible in our experiments. The role of NH_x species during deposition may be investigated further by carrying out the deposition from $TMA/N_2/H_2$ mixtures.

Films and powders of AlN are successfully deposited using TMA and NH_3. Higher pressures, lower TMA/NH_3 ratios, and lower temperatures favor particle deposition over film formation. Particle nucleation may proceed homogeneously or heterogeneously. A heterogeneous nucleation mechanism has been proposed for silicon nitride powder formation in low-pressure plasmas (Anderson et al., 1990). Film formation on electrode surface, followed by electron impact desorption of surface clusters and subsequent ionization and molecular reaction with ions has been proposed by Anderson et al. for silicon nitride particle formation.

Table 3. RF Plasma-Deposited Powder Properties

Particle size	$1.0\text{–}2.0 \times 10^{-8}$ m (10–20 nm)
Crystallinity	Amorphous
Surface area	85 m^2/g
Purity	Amine impurities escape upon heating No IR-detectable O_2

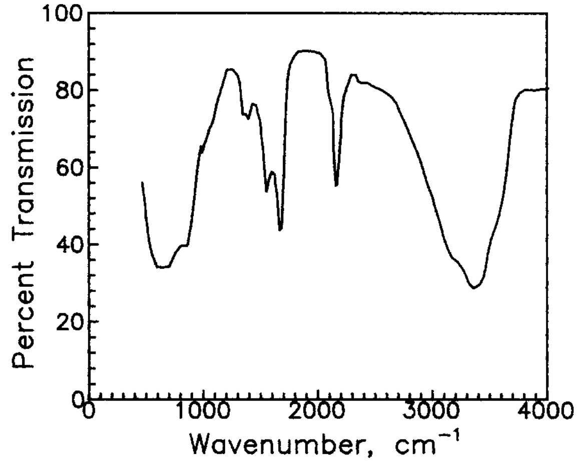

Figure 6. IR spectrum of as-deposited aluminum nitride powder.

Some key differences in the experimental results between silicon nitride and aluminum nitride depositions may be noted. In silicon nitride deposition, a lag time between initiation of the plasma and the occurrence of scattered light intensity has been observed, whereas no such induction period is observed in the present study. Anderson et al. attribute this lag to the time taken for initial film formation, which is a necessity for nucleation in their proposed mechanism. Another difference is in the particle growth process. According to their mechanism, particles grow continuously to a size determined by the residence time in the plasma, while the particle number density remains approximately constant. In the present study, the particle size is found

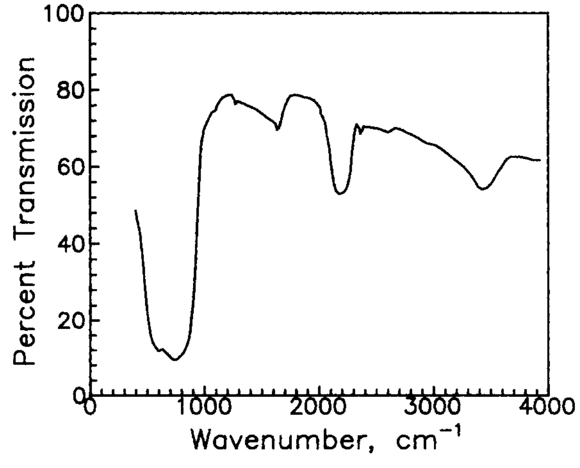

Figure 7. IR spectrum of RF plasma-deposited aluminum nitride powder heat treated at 600°C for 6 h.

to be invariant with deposition time, while the number of particles increases continuously. These differences suggest that the nucleation and growth mechanism may be different in the two cases.

The contribution of heterogeneous processes to deposition may be assessed by comparing the "specific energy" (eV/molecule) (Kline, 1989, p. 54) supplied as RF power. If the energy supplied is inadequate, then surface-catalyzed processes must be helping to overcome energy bottlenecks during deposition. The contribution of heterogeneous processes to deposition may be assessed by comparing the specific energy required for depositing the powder with the actual specific energy supplied as RF power. Unfortunately, in the present case the energy supplied by the RF power (~14 eV/molecule) exceeds the energy required for complete dissociation and reaction of the reactant gases to form the deposition product by close to a factor of three. Thus, the need for surface catalyzed processes cannot be determined. Experiments with lower input power are needed to determine whether such high specific energies are required for powder formation.

Higher pressures facilitate homogeneous gas phase nucleation of particles due to more frequent gas phase collisions. Furthermore, lower temperatures cause higher supersaturations that lead to particle formation. Film formation requires higher temperatures due to the necessity for the occurrence of surface reactions. For instance, in plasma-enhanced CVD of AlN from aluminum bromide and mixtures of nitrogen and hydrogen or argon (Itoh et al., 1987), a surface reaction between NH_x^+ and aluminum bromide has been proposed to occur. Itoh et al. also report that below a substrate temperature of 480°C, most of the deposited film consists of NH_4Br. A surface reaction between amine (NH_x) species and TMA is likely in the present system also, but without the formation of any nonvolatile contaminant, as shown by the IR spectrum in Figure 3. The deposition rate at 250°C is comparable to that reported by Itoh et al. when the NH_4Br weight is subtracted. Since film deposition requires a higher TMA/NH_3 ratio, the sticking coefficient of TMA presumably limits the film deposition rate at this temperature.

Deposited films of AlN are amorphous and pure, with a high band gap, in agreement with the reported results (Hasegawa et al., 1987). The amorphous PECVD films of aluminum nitride grown here have smoother surface morphologies when compared to the films deposited by CVD techniques, making them superior as optical coatings. The reflectance measurements of the plasma-deposited AlN films in the extreme UV wavelength region also indicate a high band gap film. The high reflectivity and the extremely smooth surface of these films combined with the advantage of very low deposition temperatures make them potentially strong candidates for antireflection coatings over optical components at the vacuum UV wavelengths.

Low-pressure RF plasma-deposited powders of AlN are fundamentally different from those deposited by other techniques such as nitridation of aluminum and alumina powders and high-pressure vapor phase synthesis methods. Nonthermal plasma-deposited powders have extremely small particle size and high surface area, very similar to RF plasma-deposited silicon nitride powder (Ho et al., 1989). The primary reason for the difference in powder properties is the low deposition temperature where high supersaturations and low atom mobilities prevail. Under these conditions, contamination of the powder by the plasma-produced amines and others is an important concern, especially due to the relatively large surface area. Nevertheless, amine impurities in the precursor powder may be beneficial due to their ability to scavenge residual water and oxygen (Soni, 1988) during controlled atmosphere sintering. In any case, the amine impurities themselves escape from the powder at the end of heat treatment, as indicated by the IR spectral measurements, shown in Figure 7.

Finally, several questions regarding the deposition mechanism for aluminum nitride in TMA/NH_3 plasmas remain unanswered. Of particular importance is the issue of homogeneous vs. heterogeneous nucleation.

Acknowledgment

This research is supported by the Center for Advanced Materials Processing (CAMP) at Clarkson University through a grant from the New York State Science Foundation. The authors thank Bruce K. Flint of Acton Research Corporation for the UV reflectance measurements. The authors thank H. M. Anderson for providing a preprint of his paper (Anderson et al., 1990).

Literature Cited

Anderson, H. M., T. T., Kodas, and D. M. Smith, "Vapor-Phase Processing of Powders: Plasma Synthesis and Aerosol Decomposition," *Ceram. Bull.*, **68,** 996 (1989).

Anderson, H. M., R. Jairath, and J. L. Mock, "Particulate Generation in Silane/Ammonia RF Discharges," *J. Appl. Phys.* (May, 1990).

Baba, K., N. Shahota, and M. Yonezawa, "Synthesis and Properties of Ultrafine AlN Powder by RF Plasma," *Appl. Phys. Lett.*, **54,** 2309 (1989).

Collins, A. T., E. C. Lightowers, and P. J., Dean, "Lattice Vibration Spectra of Aluminum Nitride," *Phys. Rev.*, **158,** 833 (1967).

Eichhorn, G., and U. Rensch, "MOCVD of AlN on Silicon," *Phys. Stat. Sol. (a)*, **69,** K3 (1982).

Handbook of Chemistry and Physics, 66th ed., "IR Correlation Chart," CRC Press, Boca Raton, Fl, F-199 (1985).

Hasegawa, F., T. Takahashi, K. Kubo, and Y. Nannichi, "Plasma CVD of Amorphous AlN from Metalorganic Al Source and Properties of Deposited Films," *Japan. J. Appl. Phys.*, **26,** 1555 (1987).

Heavens, O. S., *Optical Properties of Thin Solid Films*, Dover, New York (1965).

Hirose, M., in *Plasma-Deposited Thin Films*, J. Mort, F. Jansen, eds. CRC Press, Boca Raton, FL (1986).

Ho, P., R. J. Buss, and R. E. Loehman, "Glow Discharge Synthesis of Silicon Nitride Precursor Powders," *J. Mat. Res.*, **14,** 873 (1989).

Itoh, H., M. Kato, and K. Sugiyama, "Plasma-Enhanced Chemical Vapor Deposition of AlN Coatings on Graphite Substrates," *Thin Solid Films*, **146,** 255 (1987).

Kline, L. E., in *Plasma Etching*, J. R. Burke, ed., Semiconductor Research Corp., Research Triangle Park, NC (1989).

Lowell, S., *Introduction to Powder Surface Area, Wiley*, New York (1979).

Rensch, U., and G. Eichhorn, "Investigations on the Structure of MOCVD AlN Layers on Silicon," *Phys. Stat. Sol (a)*, **77,** 195 (1983).

Sakai, T., M. Kuriyama, T. Inukai, and T. Kizima, "Effect of Oxygen Impurity on the Sintering and the Thermal Conductivity of AlN Polycrystal," *J. Ceram. Soc. Japan*, **86,** 174 (1978).

Sheppard, L. M., "Vapor-Phase Synthesis of Ceramics," *Adv. Matls. Processes*, **53** (1987).

Soni, P. L., *Textbook of Inorganic Chemistry*, 18th ed., Sultan Chand, New Delhi, India, (1988).

Werdecker, W., and F. Aldinger, "Aluminum Nitride—An Alternative Ceramic Substrate for High-Power Applications in Microcircuits," *IEEE Trans. Cmpn., Hybd., and Mfg. Technol.*, **CHMT-7,** 399 (1984).

Manuscript received Jan. 12, 1990, and revision received Apr. 4, 1990.